XI National and II International Engineering Thermodynamics Congress

Paper Number: 29146

Innovative, detailed methodology to obtain the PV potential of industrial roofs on a regional scale

Joan D. Viana-Fons[1*], José Gonzálvez-Maciá[1], Salvador Seguí-Chilet[2], Jorge Payá[1]

Universitat Politècnica de València, Camino de Vera s/n, 46022 València, Spain.
[1]Instituto Universitario de Investigación de Ingeniería Energética (IUIIE), Ed 8E, Semisótano frente Acceso J.
[2]Electronic Engineering Department (DIE), Ed 7F, Planta 3.

*Corresponding author. E-mail address: jviana@iie.upv.es

ABSTRACT

This paper presents a systematic GIS-based approach to analyze the impact of PV panels on a regional scale. This study is based on geographic and meteorological information on a regional scale (10^6-10^{10} m^2) using models which are employed in architecture scale (10^2-10^6 m^2) and which are applied using GIS systems. The assessed region is the valencian community "l'Horta" located in the east of Spain.

The starting point in the methodology is to use geographic information to obtain the 3D model of the existing buildings by means of clustering algorithms. The weather data from different satellite and terrestrial sources is used in order to obtain a Typical Meteorological Year (TMY). The 3D model of the industrial roofs and the available radiation (TMY file) help calculate the effective solar irradiance on the roofs. The PV power output is obtained using a cell-string level PV module model, an inverter model and a Maximum Power Point Tracker (MPPT) model. A genetic algorithm enables the maximization of the annual PV energy output given the orientation of the roofs.

The model provides relevant outputs such as the PV efficiency, total PV energy output, the economic analysis or environmental impact. The mentioned methodology has been programmed in R and is applicable to other regions and can help select the most interesting locations for PV according to energy, economic and environmental criteria on a regional scale.

Keywords: *Solar energy, GIS-based approach, Photovoltaics potential assessment, LiDAR*

1. Introduction

The electrical system in Spain has to be prepared for very high levels of photovoltaic penetration and it is expected that a large part of it will be from distributed generation. This type of production is presented as the future of a large part of electricity generation worldwide and is already part of the road map of all actors, aimed at exploiting its main advantages and opportunities: management of the intermittency of sources of variable energy and minimization of losses through flexible demand and distributed storage [1].

In order to develop and implement this type of electrical generation, useful tools with the sufficient accuracy and spatial extension are necessary for planning and managing these grids. In this context, the GIS-based applications and the use of remote sensing, as LiDAR, are a common approach to address this issue. Thus, many methods have been proposed using remote sensing data to estimate the solar resource [2–5]. Likewise, various nonlinear models have been developed and applied from GIS environments to estimate the photovoltaics potential [6, 7] and their economic and environmental impact [8].

This paper presents a novel methodology that integrates four detailed models – the 3D-vector building model, their roof's solar resource, their photovoltaic potential and their economic and environmental impact – with a high level of accuracy and applied to large areas using Geographic Information Systems (GIS). The level of detail of the employed models enables working with georeferenced hourly time series and helps to perform the optimum sizing and orientation of each pair module/inverter for each roof according to energy, economic and environmental criteria and based on specific operating points of the considered devices.

2. Methodology

The proposed methodology consists in the integration of four coupled models (Figure 1) that, starting from geographical and meteorological data, helps to obtain the 3D model of the existing industrial buildings, by means of clustering algorithms, and the Typical Meteorological Year (TMY) of the studied area. Based on the roof orientations and the available radiation, the effective solar irradiance is obtained by considering the shading and angular losses. Then, the PV power output on each roof is calculated using a cell-string level PV module model, an inverter model and a MPPT model. Finally, the economic and environmental impact of the PV generators throughout their useful lifetime are estimated. A genetic algorithm enables the optimization of the generator – i.e. pair module/inverter –, by means of sizing and orientation, according to energy, economic and environmental criteria given the orientation of the roofs.

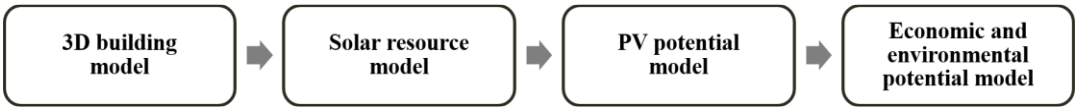

Figure 1. Workflow of the developed methodology

A more detailed explanation of these models, analyzed individually in four sections, is included below.

2.1 3D building model

A GIS-based model has been developed in order to detect and characterize the industrial roofs of the studied area. As a result, a set of coplanar polygons, characterized by their dimensions and orientation (tilt and azimuth), have been obtained.

Following the scheme shown in Figure 2, the footprints of the industrial buildings are obtained from the cadastral map and the land cover map. Once the outline of the target constructions is collected, the related LiDAR (Light Detection and Ranging) point clouds of each individual building are extracted and analyzed.

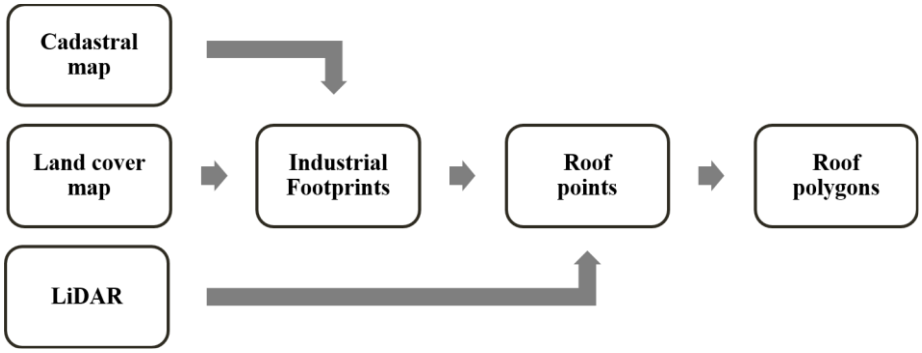

Figure 2. Workflow of the proposed 3D building model

A set of algorithms have been developed to detect, segment and classify the building's roof typology (flat, sloped, saw-type, gabled or curved) from the roof's point cloud, according to the orientation of

their different coplanar entities. Firstly, a set of filters of minimum footprint area, minimum number of points and minimum density of points are applied. Then, flat roofs are detected by the height difference between the 10th and 90th percentile of the Z coordinate and by the evaluation of the linear regression of its coordinates XZ and YZ. Thereafter, the tilt and azimuth are obtained for each roof point using the model developed by Horn [9]. Finally, the k-means clustering algorithm is applied to segment the different roof typologies in coplanar entities obtaining a vector-based 3D model of the studied area.

2.2 Solar radiation model

Firstly, the Typical Meteorological Year (TMY) of the studied area is calculated using the procedure presented by Wilcox and Marion [10] using long term data from satellite and terrestrial meteorological stations. The hourly data of the direct $B(0)$ and diffuse $D(0)$ horizontal irradiance components are collected from satellite data source in the centroid of the studied area for a period of 15 years (2002-2016). Hourly data for dry-bulb temperature T, relative humidity HR, wind speed v and global horizontal irradiance $G(0)$ are collected from three terrestrial stations, placed at least 15km far from the centroid of the studied area, for the same period than the satellite data. The data of the variables used for each month is selected, between the three terrestrial stations considered, using those that minimizes the global monthly irradiation differences between the terrestrial and the satellite data.

Once the TMY is obtained, typical models of solar geometry [11, 12] and radiation [13, 14] are used to obtain the hourly time series of the three components (direct, diffuse and reflected) of the solar irradiance $G(\alpha, \beta)$ incident on a surface – i.e. PV module – as a function of its orientation α, β.

Then, a geometric shading model between modules is used for each component of the radiation, defined with respect to the solar azimuth ψ_s, the solar elevation γ_s, the orientation of the modules α, β and the orientation of the roof α_R, β_R. For the diffuse and reflected components the mask angle concept is applied [15, 16] while for the direct component the shadow factor F_{sha} is calculated using a geometric model. Thus, considering the distance between modules d, the shadow length on the module surface can be calculated as $s_m = F_{sha} \cdot (s - d)$, where s is the shadow length on the roof surface.

Finally, the losses by angular effects F_{ang} are estimated using the model developed by Martin and Ruiz [17] considering a mid-degree of dirtiness of the modules.

Considering the previous approach, the total effective irradiance per unit of roof surface G_{ef} is finally calculated as a function of module and roof orientation.

2.3 Photovoltaics model

For this model, four commercial crystalline silicon photovoltaic modules (Table 1) and five commercial three-phase inverters (Table 2) with different nominal power were considered. The devices were selected considering the technology's market share, the availability of data and the proximity of the manufacturers and suppliers.

For the PV modules, the cell level model at STC (Standard Test Conditions) proposed by Batzelis and Papathanassiou [18] is used to obtain the five parameters of the single-diode model for each module from the typical commercial datasheets. According to the module layout, a cell-string level model is considered as a series connection of the cells protected by each bypass diode. Using the shading time series of each radiation component, the spectral response F_{spe} is calculated for each cell string using the model developed by Martin and Ruiz [19]. Likewise, the cell temperature is estimated using the Duffie and Beckman model [14]. Therefore, the five parameters of the single-diode model at non-standard conditions can be calculated using the Ruiz model [20] and the I-V and P-V curves of each module can be obtained using the model desbribed by Batzelis et. al [21]. Finally, the strategy of activation of the bypass diodes is selected in order to maximize the power output of the modules according to the MPPT (Maximum Point Power Traking) algorithm.

Table 1. Atersa's PV modules considered for this study

Model	Technology	N_{cell}	P_n (kW)	TONC (ºC)	W (m)	L (m)	F_{deg} (%)
Atersa A-255M	Mono-c-Si	60	255	47	0.99	1.64	0.68
Atersa A-275M	Mono-c-Si	60	275	47	0.99	1.64	0.68
Atersa A-315P	Poly-c-Si	72	315	47	0.99	1.97	0.68
Atersa A-330M	Mono-c-Si	72	330	47	0.99	1.97	0.68

For the inverters, the Jantsch model introduced by Rampinelli [22] is used. With this model, the inverter efficiency η_I is defined by means of six coefficients as a function of its charge and input voltage. In order to obtain these coefficients from the typical commercial datasheets of each inverter, firstly three charge-dependent coefficients are obtained solving a non-linear least squares problem of the Gauss-Newton algorithm. Secondly, the final six coefficients are calculated solving three linear least squares problems by the QR algorithm.

Table 2. SMA's inverters considered for this study

Model	P_n (kW)	P_{max} (kW)	V_{DC} (V)	V_{MPPT}^{max} (V)	V_{MPPT}^{min} (V)
SMA Sunny Tripower 12000TL	12	18.00	580	800	440
SMA Sunny Tripower 25000TL	25	25.55	600	800	390
SMA Sunny Tripower 60	60	61.24	630	800	570
SMA Sunny Central 760CP XT	836	853.00	577	850	480
SMA Sunny Central 1000CP-XT	1100	1122.00	688	850	596

An algorithm of MPPT is used to consider the power losses F_{MPPT} when the array voltage are out of the tracker range and the current of the strings are imposed. In such cases, the I-V and P-V curves of the modules are considered to select the voltage and the bypass diodes connections that maximize the total power of the generator.

Finally, other losses of Balance of System (BOS) are assumed as fixed values. The latter include a factor of module power tolerance F_{man}, ohmic losses factors F_{DC} and F_{AC} at DC and AC circuits respectively, mismatch losses F_{mis} and transformer losses F_{tra}.

To sum up, the voltage V_{DC}, current I_{DC} and power P_{DC} time series of the PV array are defined as:

$$\begin{aligned} I_{DC} &= I^m \cdot N_{mp} \cdot \sqrt{1 - F_{MPPT}} \cdot \sqrt{1 - F_{man}} \cdot (1 - F_{mis}) \\ V_{DC} &= V^m \cdot N_{ms} \cdot \sqrt{1 - F_{MPPT}} \cdot \sqrt{1 - F_{man}} \cdot (1 - F_{DC}) \\ P_{DC} &= I_{DC} \cdot V_{DC} \end{aligned} \quad (1)$$

Denoting V^m, I^m as the voltage and current of the module and N_{ms}, N_{mp} the number of modules per string and number of strings, respectively.

Based on this PV array power model, the inverter efficiency and the electrical DC circuit's limits imposed by the inverter, a non-linear programming problem is proposed for sizing – i.e. obtain N_{ms}, N_{mp} – each generator in order to optimize its productivity, according to the orientation and the considered devices.

$$\text{Maximize} \quad E_{AC} = \frac{\sum_{t=1}^{8760} \eta_I(t) \cdot P_{DC}(t)}{N_{ms} \cdot N_{mp}}$$

Subject to:

$$N_{ms} \leq \frac{V_{max}^{i,MPPT}}{V_{mp}|_{max}} \quad N_{ms} \geq \frac{V_{min}^{i,MPPT}}{V_{mp}|_{max}} \quad N_{ms} \leq \frac{V_{max}^{i}}{V_{oc}|_{max}}$$

$$N_{mp} \leq \frac{I_{max}^{i}}{I_{sc}|_{max}} \quad N_{mp} \leq \frac{I_{max}^{i,MPPT}}{I_{mp}|_{max}} \quad N_{ms} \cdot N_{mp} \leq \frac{s \cdot P_n}{P_{mp0}} \qquad (2)$$

$$s \in [1.1,1.5] \qquad N_{ms}, N_{mp} \in \mathbb{Z}^+ \qquad P_{DC}(t), \eta_I(t) \in \mathbb{R}^{8760}$$

$$P_n, V_{max}^{i,MPPT}, V_{min}^{i,MPPT}, I_{max}^{i,MPPT}, V_{max}^{i}, I_{max}^{i} \in \mathbb{R}^+$$

$$V_{mp}|_{max}, P_{mp}|_{max}, I_{mp}|_{max}, I_{sc}|_{max}, V_{oc}|_{max} \in \mathbb{R}^+$$

In the previous equations, s is the oversizing ratio of the PV array and the worst-case scenarios have been considered for the electrical constraints using the extreme values of temperature and solar irradiance of the studied area.

The optimization problem is solved by the version of the Genetic Algorithm *Genetic Optimization Using Derivatives* described by Sekhon and Mebane [23]. The results are obtained for twenty generators as a combination of the four modules and the five commercial inverters considered.

2.4 Economic and environmental model

Starting from the PV's power hourly time series of the representative year (TMY) on each roof of the studied area, the corresponding time series throughout the useful lifetime of the generators are calculated considering the annual degradation factor provided by the manufacturer (Table 1) and the life expectancy recommended by the IEA [24].

On the one hand, the hourly data of energy price at wholesale market, primary emissions and primary energy of the mix are obtained from the grid operator. In order to estimate the values of these variables during the whole life cycle, a prediction model has been adopted. Thus, starting as training-data the hourly time series of two years period (2015-2016) a regression model has been estimated for each variable using Support Vector Machines, more specifically the *Support Vector Regression* (nu-SVR) formulation, implemented in the e1071 R package [25], using only variables related to time (month, day of week and hour) as predictors. The results of the regression are corrected with the expected inflation and the evolution of the grid's emissions and primary energy consumption.

On the other hand, the corresponding feed-in-tariff (FIT) is estimated throughout the lifetime according to the regulations of grid connected PV systems in Spain (RDL 9/2013), which are inspired in the concept of *reasonable profitability*, based on the average yield (pre-tax) of Spanish 10-year government bonds plus 300 basis points.

Based on market prices, projections and regulations, the total revenues are estimated and the total investment and operating costs are assumed according to the values reported in Table 3.

Table 3. Economic data assumptions for the first year

IC (€/kWn)	OC (€/kWn·year)	R (€/kWn·year)	Loan (% IC)	Loan IR (%)
1606.21	77.52	190.30	70.00	3.35

IC : Investment Costs ; **OC** : Operation Costs ; **IR** : Revenue ; **IR** : Interest rate

Using the reported data, a Payback and an economic analysis has been made in order to obtain, for the twenty generators, the following main indicators: the Net Present Value NPV, the Discounted Payback Period DPP, the Internal Rate of Return IRR, the Return on Assets ROA and the Return on Equity ROE.

Similarly, an environmental Payback has been made in order to calculate the Carbon Payback Period CPBT and the Primary Energy Payback Period PEPP. For this analysis, the primary energy required and the emissions associated with manufacture, transportation, operation and dismantling of facilities, have been estimated according to the data shown in Table 4, based on the Life Cycle Analysis [26–28]. Furthermore, the emission and the final energy conversion factors to primary energy of the grid's energy mix has been considered according to IDAE [29].

Table 4. Primary energy required and the emissions associated to the Life Cycle Analysis of the PV generators

	E_{LCA} (MJ/kW_p)	C_{LCA} (kg_{CO2}/kW_p)
Modules	43914	1482
Inverter	1154	40
Other BOS	1089	26

Based on these economic and environmental models, the non-linear programming problem proposed for sizing is formulated in order to maximize economic or environmental returns.

3. Results and discussion

The previous methodology has been applied to an area of 723.47 km^2, in the valencian community "l'Horta" located in the east of Spain. The total constructed area of industrial land is 15.18 km^2 with 25163 constructions.

3.1 3D building model

The set of dissociated polygons of coplanar industrial roof entities of each construction were obtained (**¡Error! No se encuentra el origen de la referencia.**) as a result of the GIS-based model. Considering the basic industrial roof typologies – i .e. flat, sloped, saw-type, gabled and curved –, the model correctly discriminated between all of them except for the last case, which was approximated to flat surfaces.

A representative sample was selected to validate the model considering a binomial distribution (correct / incorrect roof typology classification). The results of the sample were validated using 3D Google Maps obtaining the confusion matrix shown on the **¡Error! No se encuentra el origen de la referencia.**.

Table 5. Confusion matrix of roof typology classification for a sample size of 246 using a level of significance of 0.05 and a test power of 95%.

		Actual				
		Filtered	**Flat**	**Sloped**	**Gabled**	**Curved**
Predicted	**Filtered**	35	0	0	0	0
	Flat	0	34	0	2	0
	Sloped	0	2	27	3	0
	Gabled	0	0	0	138	3
	Curved	0	0	0	0	0

Therefore, the model had a global efficiency above 90%, both in the number and in the modeled area, with a confidence level of 0.9988.

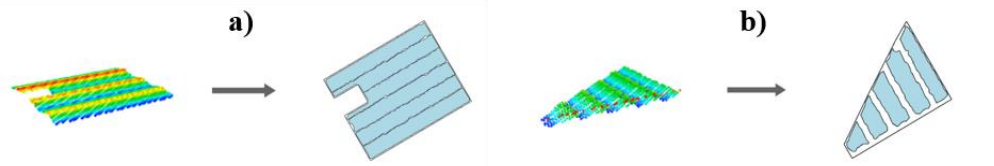

Figure 3. 3D building model results as segmented coplanar entities. a) Multiple gabled roof and b) Saw-type roof

3.2 Solar radiation model

The Typical Meteorological Year was constructed selecting for each month the data from the most representative year, obtaining the monthly solar horizontal irradiation components, the mean temperature and wind speed reported in Table 6.

Table 6. Typical Meteorological Year obtained for the studied area

Month	Year	G(0) (kWh/m^2)	D(0) (kWh/m^2)	B(0) (kWh/m^2)	T (ºC)	v (m/s)
January	2015	2.881	0.928	1.953	12.97	1.84
February	2011	3.597	1.514	2.083	13.75	1.89
March	2014	4.831	1.854	2.977	15.46	2.14
April	2009	6.012	2.701	3.311	16.40	1.68
May	2010	7.213	2.635	4.578	19.40	1.57
June	2009	7.929	2.821	5.108	24.93	1.62
July	2009	7.666	2.140	5.526	26.86	1.54
August	2015	6.317	1.989	4.328	27.23	1.58
September	2015	4.946	2.145	2.801	23.14	1.35
October	2009	4.020	1.458	2.562	20.94	1.32
November	2012	2.282	1.278	1.004	15.37	1.37
December	2006	2.160	0.962	1.198	12.36	1.55
Annual		**4.996**	**1.868**	**3.128**	**19.10**	**1.62**

The solar irradiation and the temperature results are very similar to the long term values corresponding to the city of Valencia [30, 31], with relative errors of 0.20% and 3.39%, respectively.

The total effective irradiance per unit of roof surface G_{ef}, as a function of module orientation α, β, were calculated obtaining maps (Figure 4) for each roof orientation α_R, β_R.

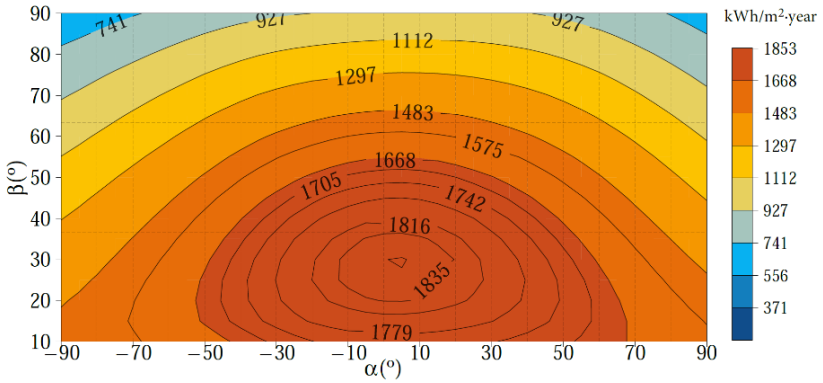

Figure 4. Map of annual effective irradiation per unit of roof surface G_{ef}, as a function of the module orientation α,β, for the roof orientation α_R,β_R=(30,10)º.

The optimal orientation in the extension of this study was found to be $\alpha_{opt}, \beta_{opt} = (0,30)°$, with a total of 1848.28 kWh/(m^2·year). It was symmetric about the azimuth, since the territory is flat, without orographic accidents. This orientation maximizes the effective annual in captured by a thermal or photovoltaic solar panel in a flat roof using the minimum distance between strings that ensures four hours without shadow in winter solstice.

3.3 Photovoltaics model

In order to evaluate the photovoltaics potential of the studied area three performance parameters were used according to Pless et al. [32]: PV system yield Y_f, Performance ratio PR and generation effectiveness GE. Table 7 collects the optimal sizing and the main representative parameters of the PV system, for each pair module/inverter considered, fixing the module and the roof orientation.

Table 7. PV energy oputput, efficiencies and sizing for all the devices considered in this study

Mod	Inv	Y_f (h)	E_{AC} (MWh)	PR	GE	η_I	F_{MPPT}	N_{ms}	N_{mp}
M_1	I_1	1477	20.3	0.782	0.122	0.972	0.059	18	3
M_2	I_1	1502	22.3	0.795	0.134	0.972	0.046	18	3
M_3	I_1	1510	21.4	0.800	0.129	0.972	0.045	15	3
M_4	I_1	1511	22.4	0.800	0.136	0.972	0.045	15	3
M_1	I_2	1484	45.4	0.786	0.123	0.975	0.057	24	5
M_2	I_2	1489	47.1	0.788	0.133	0.975	0.058	23	5
M_3	I_2	1500	44.9	0.794	0.129	0.975	0.054	19	5
M_4	I_2	1500	47.0	0.794	0.135	0.975	0.055	19	5
M_1	I_3	1496	100.6	0.792	0.124	0.983	0.058	24	11
M_2	I_3	1500	104.3	0.794	0.134	0.983	0.058	23	11
M_3	I_3	1511	108.5	0.800	0.130	0.983	0.055	19	12
M_4	I_3	1512	104.3	0.800	0.136	0.983	0.056	19	11
M_1	I_4	1463	1352.3	0.775	0.121	0.983	0.055	24	151
M_2	I_4	1469	1356.7	0.778	0.131	0.983	0.055	23	146
M_3	I_4	1477	1361.5	0.782	0.127	0.983	0.053	19	154
M_4	I_4	1479	1363.5	0.783	0.133	0.983	0.053	19	147
M_1	I_5	1389	1632.2	0.735	0.115	0.986	0.105	24	192
M_2	I_5	1432	1676.7	0.758	0.128	0.986	0.080	23	185
M_3	I_5	1477	1759.6	0.782	0.127	0.985	0.055	20	189
M_4	I_5	1452	1675.7	0.769	0.130	0.986	0.073	19	184

Inverters : I_1 = SMA 12000TL; I_2 = SMA 25000TL ; I_3 = SMA 60 ; I_4 = SMA 760XT CT ; I_5 = SMA 1000XT CT
Modules : M_1 = A-255M ; M_2 = A-275M ; M_3 = A-315P ; M_4 = A-330M

The overall performance of most of the device combinations were very similar. The only pairs with significant losses observed were A-255M/1000XT-CT and A-275M/1000XT-CT, due to the higher MPPT losses (8% and 10% respectively), because of the long time periods when the PV array voltage is not within the operating range of the MPPT tracker.

Therefore, the optimal module orientation that maximizes the electrical energy injected into the grid depends on the considered devices and on the roof orientation. The optimal orientation in a flat roof, both the average and the most common case for the twenty generators studied, were $\alpha_{opt}, \beta_{opt} = (0,34)°$, with a yield Y_f of 1501 hours, a performance ratio PR of 0.806 and a generation effectiveness GE of 0.132.

3.4 Economic and environmental model

The series of electricity injected into the grid throughout the useful lifetime of all twenty generators were calculated using different annual degradation factor values and all the economic and environmental indicators were calculated (Table 8).

Table 8. Economic and environmental parameters for different F_{deg} for the devices A-315P / 1000XT-CT

F_{deg} (%)	Y_f (h)	NPV (€)	DPP (y)	IRR (%)	ROA (%)	ROE (%)	PEPBT (y)	CPBT (y)
-0.5	1363	81310	15.7	5.5	6.3	24.2	4.8	3.2
-1.0	1270	6687	16.2	5.1	6.1	24.3	5.2	3.3
-1.5	1186	-61914	16.7	4.8	5.9	24.5	5.5	3.5

The optimal sizing depends on both the system and the pursued objective, although the results for the economic objective and for the environmental objective they were very similar to the corresponding ones for the productivity of the previous section.

The optimal orientation that maximizes the profitability of the investment depends on the considered devices. The most common case for the twenty generators, in a flat roof and $F_{deg} = 0.7$, were $\alpha_{opt}, \beta_{opt} = (0,33)°$, with a ROA of 6.17% and a ROE of 23.70%. The symmetry with respect to the azimuth as maintained, so that the hourly variation of the price of the electricity market was not significant in the return on investment. The optimum elevation for coplanar modules – i.e. the modules rest directly on the roof – increased to 38º, four more than in the solar resource and the photovoltaic potential, so that the seasonal pointing of the market price – i.e. in winter is higher – influenced the profitability of the investment.

Likewise, the orientation that optimized the environmental returns varied depending on the devices. The most common case for the studied twenty generators, in a flat roof and $F_{deg} = 0.7$, were $\alpha_{opt}, \beta_{opt} = (0,30)°$ to maximize both emissions avoided and primary energy saved, whereby CPBT = 3.34 years and PEPBT = 5.10.

3.5 Global results

The overall industrial buildings of the study were classified by their topology: flat, sloped, gabled (which includes saw-type) or curved. The last topology number and area was estimated from the representative sample. As a result of filtering and classification, 26471 coplanar entities with a total effective area of 7.82 km^2 were obtained (Table 9).

Table 9. Roof number and area obtained for the studied area using the 3D building model

Typology	N	A (km^2)	%N	%A
Flat	3581	1.23	13.53	15.79
Sloped	807	0.21	3.05	2.73
Gabled	21760	6.27	82.20	80.19
Curved	323	0.11	1.22	1.28
Total	26471	7.82	100.00	100.00

The predominant typology was gabled roof, accounting for more than 83% of the total classified cases and 80% of the effective area. The second most common typology was flat, which involves 14% of the surfaces and 15% of the area. Finally, the sloped and curved typologies added up to 3% and 1%, respectively.

The subset formed by the south-facing roofs ($\in [90, 90]°$) and the flat roofs amounted to 15092 entities and covered 4.66 km^2, maintaining the relative proportions between different typologies. The predominant orientations of the resulting surfaces, within the considered range, were concentrated in $\alpha \in [-90, -60]°$ (30%) and $\alpha \in [0, 30]°$ (25%), with a predominant elevation $\beta \in [11, 13]°$.

Therefore, the annual solar resource, photovoltaics potential throughout the useful lifetime and their economic and environmental potential were calculated for all the south facing roofs of the studied area, classified by roof typology (Table 10) and optimized according to economic criteria. The productive PV potential during its lifetime was estimated at 11.77 TWh, with a net economic potential of 230.19 M€, a potential saving of 4.74 MT_{CO2} of emissions and 16.50 MBEP of primary energy.

Table 10. Global results for the PV generators on the south-facing roofs of the studied area throughout their useful lifetime. G_{ef} is calculated using the optimal orientation for maximize the PV production. PV potential E_{AC}, total net profit NP, emissions avoided C_{mix} and primary energy saved E_{mix} are calculated using a degradation factor F_{deg} of 0.7%/year and the average values of generation effectiveness of the twenty generators optimized according to economic criteria

Typology	**$\lvert\alpha_R\rvert$**	**N**	**S (Ha)**	**G_{ef} (GWh/y)**	**E_{AC} (TWh)**	**NP (M€)**	**C_{mix} (MT_{CO2})**	**E_{mix} (MTEP)**
Flat		2587	116.73	864.94	1.86	45.34	0.75	2.61
Gabled	**≤ 30**	3253	124.29	1417.87	3.00	73.23	1.21	4.21
Sloped	**≤ 30**	147	5.63	60.82	0.13	3.15	0.05	0.18
Gabled	**∈ (30,90]**	4914	191.73	2750.98	6.58	105.17	2.65	9.22
Sloped	**∈ (30,90]**	176	5.71	83.36	0.20	3.30	0.08	0.28
Total	**∈ [0,90]**	11077	444.10	5177.98	11.77	230.19	4.74	16.50

To manufacture, transport, exploit and dismantle these generators it was estimated that, according to the life cycle analysis, 3.52 MBEP of primary energy were required with associated emissions of 0.65 MT_{CO2}, recoverable in 6.44 and 4.15 years, respectively.

The amount of energy was estimated to cover 12% of the total consumption of these buildings. According to the typology and the orientation of the surfaces, an average annual potential across their lifetime of 61 GWh/year over flat roofs and 219 GWh/year over south gabled roods were estimated. Therefore, 48% of the potential was concentrated in roofs of less than 500 m^2, while 23% is concentrated in 722 roofs of more than 1000 m^2.

4. Conclusions

This document proposed a systematic and programmable methodology, applied from Geographic Information Systems (GIS), which integrates four detailed models that, beginning with the 3D model of the existing buildings, enables to simulate and obtain, precisely, the solar resource and the photovoltaic potential, as well as its associated economic and environmental potential on a regional scale.

The level of detail of the employed models allows to obtain a set of georeferenced hourly time series throughout the useful lifetime of the generators and enables to perform the optimum sizing and orientation of each pair module/inverter for each roof according to energy, economic and environmental criteria and based on specific operating points of the considered devices.

The assessed region is the valencian community “l’Horta” located in the east of Spain and applied to industrial buildings. The results showed that the solar resource of the industrial south facing roofs of the studied area is around 5178 GWh/year distributed in 11077 coplanar surfaces using a total area of 444.1 Ha and the corresponding PV average potential, across their lifetime, is around 392 GWh/year, with a

net economic potential of 7673 k€/year, a potential saving of 158 kT_{CO2}/year of emissions and 550 kBEP/year of primary energy.

The proposed methodology is applicable to most regions and land uses, where LiDAR and long-term meteorological data is available, in order to help select the most interesting roof locations for solar technologies.

REFERENCES

[1] SCHMALENSEE, R. *The Future of Solar Energy*. 2015.

[2] FREITAS, S; CATITA, C; REDWEIK, P; BRITO, M C. *Modelling solar potential in the urban environment: State-of-the-art review. Renewable and Sustainable Energy Reviews*. 2015, **41**, 915–931.

[3] M. MARTÍN, A; DOMÍNGUEZ, J; AMADOR, J. *Applying LIDAR datasets and GIS based model to evaluate solar potential over roofs: a review*. *AIMS Energy*. 2015, **3**(3), 326–343.

[4] REDWEIK, P; CATITA, C; BRITO, M. *Solar energy potential on roofs and facades in an urban landscape*. *Solar Energy*. 2013, **97**, 332–341.

[5] CATITA, C; REDWEIK, P; PEREIRA, J; BRITO, M C. *Extending solar potential analysis in buildings to vertical facades*. *Computers and Geosciences*. 2014, **66**, 1–12.

[6] LUKAČ, N; SEME, S; ŽLAUS, D; ŠTUMBERGER, G; ŽALIK, B. *Buildings roofs photovoltaic potential assessment based on LiDAR (Light Detection And Ranging) data*. *Energy*. 2014, **66**, 598–609.

[7] LINGFORS, D; KILLINGER, S; ENGERER, N A; WIDÉN, J; BRIGHT, J M. *Identification of PV system shading using a LiDAR-based solar resource assessment model: An evaluation and cross-validation. Solar Energy*. 2018, **159**, 157–172.

[8] LUKAČ, N; SEME, S; DEŽAN, K; ŽALIK, B; ŠTUMBERGER, G. *Economic and environmental assessment of rooftops regarding suitability for photovoltaic systems installation based on remote sensing data. Energy*. 2016, **107**, 854–865.

[9] HORN, B K P. *Hill shading and the reflectance map*. *Proceedings of the IEEE*. 1981, **69**(1), 14–47.

[10] WILCOX, S; MARION, W. *Users manual for TMY3 data sets. Renewable Energy*. 2008, (May), 51.

[11] SPENCER, J W. *Fourier Series Representation of the Position of the Sun*. 1971, **2**.

[12] WHITMAN, A M. *A simple expression for the equation of time*. *Journal Of the North American Sundial Society*. 2003, **14**, 29–33.

[13] HAY, J E; MCKAY, D C. *Estimating Solar Irradiance on Inclined Surfaces: A Review and Assessment of Methodologies*. *Int. J. Solar Energy*. 1985, (3), 203.

[14] DUFFIE, J A; BECKMAN, W A. *Solar Engineering of Thermal Processes*. B.m.: Wiley, 1991. A Wiley-Interscience Publication.

[15] PASSIAS, D; KÄLLBÄCK, B. *Shading effects in rows of solar cell panels*. *Solar Cells*. 1984, **11**(3), 281–291.

[16] GOSWAMI, D Y; STEFENAKOS, E K; HASSAN, A Y; COLLIS, W J. *Effect of row-to-row shading on the out-put of flat-plate south-facing photovoltaic arrays. Journal of solar energy engineering*. 1989, **111**(3), 257–259.

[17] MARTIN, N; RUIZ, J M. *Calculation of the PV modules angular losses under field conditions by means of an analytical model*. 2001, **70**, 25–38.

[18] BATZELIS, E I; PAPATHANASSIOU, S A. *A Method for the Analytical Extraction of the*

Single-Diode PV Model Parameters. *IEEE Transactions on Sustainable Energy*. 2016, **7**(2), 504–512.

[19] MARTÍN, N; RUIZ, J M. *A new method for the spectral characterisation of PV modules*. *Progress in Photovoltaics: Research and Applications*. 1999, **7**(4), 299–310.

[20] ALONSO-GARCÍA, M C. *Caracterización y modelado de asociaciones de dispositivos fotovoltaicos*. B.m., 2005. CIEMAT.

[21] BATZELIS, E I; KAMPITSIS, G E; PAPATHANASSIOU, S A; MANIAS, S N. *Direct MPP Calculation in Terms of the Single-Diode PV Model Parameters*. *IEEE Transactions on Energy Conversion*. 2015, **30**(1), 226–236.

[22] ARNS RAMPINELLI, G. *Estudo de características eléctricas e térmicas de inversores para sistemas fotovoltaicos conectados à rede*. B.m., 2010. Universidade Federal do Rio Grande do Sul.

[23] SEKHON, J S; MEBANE, W R. *Genetic Optimization Using Derivatives*. *Political Analysis*. 1998, **7**(1), 187–210.

[24] DONES, R; FRISCHKNECHT, R. *Life-cycle assessment of photovoltaic systems: results of Swiss studies on energy chains*. *Progress in Photovoltaics: Research and Applications*. 1998, **6**(2), 117–125.

[25] HORNIK, K; WEINGESSEL, A; LEISCH, F; DAVIDMEYERR-PROJECTORG, M D M. *Package 'e1071''.'* 2017.

[26] PERPIÑAN LAMIGUEIRO, O. *Energía Solar Fotovoltaica*. 2012, 194.

[27] HAMMOND, G P; JONES, C I. *Embodied energy and carbon in construction materials*. 2008, (May), 87–98.

[28] ENERGY, A; SIM, M De; ALONSO-TRIST, C. *Real Energy Payback Time and Carbon Footprint of a GCPVS*. 2017, (January).

[29] IDAE. *Factores de conversión Energía Final - Energía Primaria y Factores de Emsión de CO2*. 2012.

[30] SANCHO, J M; RIESCO, J; JIMÉNEZ, C; SÁNCHEZ, M C; MONTERO, J; LÓPEZ, M. *Atlas de Radiación Solar*. 2012.

[31] AGENCIA ESTATAL DE METEOROLOGÍA DE ESPAÑA. *Arcimís: Guía resumida del clima en España (1981-2010)*. 2012.

[32] PLESS, S; DERU, M; TORCELLINI, P; HAYTER, S. *Procedure for Measuring and Reporting the Performance of Photovoltaic Systems in Buildings*. 2005, (October).